HHS Public Access

Author manuscript

JACC Cardiovasc Imaging. Author manuscript; available in PMC 2016 May 01.

Published in final edited form as:

JACC Cardiovasc Imaging. 2015 May ; 8(5): 597–611. doi:10.1016/j.jcmg.2015.02.007.

Noninvasive Multimodality Imaging in ARVD/C

Anneline S.J.M te Riele, MD[*,†], **Harikrishna Tandri, MD**[*], **Danita M. Sanborn, MD**[‡], and **David A. Bluemke, MD, PhD**[§,‖]

[*]Department of Medicine, Division of Cardiology, Johns Hopkins University School of Medicine, Baltimore, Maryland [†]Department of Medicine, Division of Cardiology, University Medical Center Utrecht, Utrecht, the Netherlands [‡]Department of Medicine, Division of Cardiology, Massachusetts General Hospital, Harvard Medical School, Boston, Massachusetts [§]Department of Radiology, Johns Hopkins University School of Medicine, Baltimore, Maryland [‖]Radiology and Imaging Sciences, National Institutes of Health Clinical Center, Bethesda, Maryland

Abstract

Arrhythmogenic right ventricular dysplasia/cardiomyopathy (ARVD/C) is a familial cardiomyopathy resulting in progressive right ventricular (RV) dysfunction and malignant ventricular arrhythmias. Although ARVD/C is generally considered an inherited cardiomyopathy, the arrhythmogenic nature of the disease is striking. Affected individuals typically present in the second to fourth decade of life with arrhythmias originating from the right ventricle. Over the past decade, pathogenic ARVD/C-causing mutations have been identified in 5 genes encoding the cardiac desmosome. Disruption of the desmosomal connection system between cardiomyocytes may be represented structurally by ventricular enlargement, global or regional contraction abnormalities, RV aneurysms, or fibrofatty replacement. These abnormalities are typically observed in predilection areas, including the subtricuspid region, basal RV free wall, and left ventricular posterolateral wall. As such, structural and functional abnormalities on cardiac imaging constitute an important diagnostic criterion for the disease. This paper discusses the current status and role of echocardiography, cardiac magnetic resonance imaging, and computed tomography for suspected ARVD/C.

Keywords

arrhythmogenic right ventricular dysplasia/cardiomyopathy; cardiac magnetic resonance; computed tomography; echocardiography; imaging

Arrhythmogenic right ventricular dysplasia/cardiomyopathy (ARVD/C) is an inherited cardiomyopathy characterized by fibrofatty replacement of the right ventricular (RV) myocardium, predisposing patients to ventricular arrhythmias and usually slowly progressive ventricular dysfunction (1). The disease is inherited as an autosomal dominant

REPRINT REQUESTS AND CORRESPONDENCE: Dr. David A. Bluemke, Radiology and Imaging Sciences, National Institutes of Health Clinical Center, 10 Center Drive, Bethesda, Maryland 20892. david.bluemke@nih.gov.

The authors have reported that they have no relationships relevant to the contents of this paper to disclose.

APPENDIX For supplemental videos and their legends, please see the online version of this article.

trait with incomplete penetrance and variable expressivity (2). Although the exact prevalence of this condition is unknown, ARVD/C is recognized as a major cause of sudden cardiac death in the young and in athletes (3–5). Definite ARVD/C diagnosis is on the basis of the presence of major and minor criteria encompassing structural, histologic, electrocardiographic, arrhythmic, and family history criteria proposed by a Task Force in 2010 (Table 1) (6). Affected individuals typically present in the second or third decade of life with palpitations, lightheadedness, or syncope due to ventricular tachycardia originating from the RV (5). In addition, with the advent of genetic testing, an increasingly large group of asymptomatic mutation carriers is coming to clinical attention.

Over the last decade, ARVD/C has drawn considerable attention because of better understanding of the underlying pathophysiology, diagnostic improvements, and advanced therapeutic options. ARVD/C has been increasingly associated with mutations in genes encoding proteins involved in the desmosome apparatus (7–11). Desmosomes are specialized adhesion junctions providing mechanical connection between cardiomyocytes (12). The defective connection system in ARVD/C may be represented structurally by ventricular enlargement, global or regional contraction abnormalities, focal bulging of the RV wall in diastole, or fibrofatty replacement (13–15). Therefore, accurate evaluation of ventricular structure and function is essential for the evaluation of patients and screening of their relatives. The aim of this review is to provide a practical and current approach to noninvasive imaging for suspected ARVD/C.

IMAGING OF ARVD/C

ARVD/C may present a diagnostic challenge for the physician. In our experience, overemphasis of imaging results without reference to other ARVD/C criteria may be problematic. RV imaging abnormalities by themselves are not the “gold standard” for ARVD/C diagnosis. Rather, the diagnostic Task Force Criteria (TFC) prescribe the use of multiple diagnostic tests. In addition, many imaging centers have little or no experience with ARVD/C, and gaining experience is difficult because of the low prevalence of disease. The clinical features and associated structural findings of conditions included in the differential diagnosis of ARVD/C are described in Table 2. A more comprehensive description of ARVD/C mimics is available from Rastegar et al. (16).

Many subjects with ARVD/C are young, and the need for screening tools among genetically predisposed, but clinically asymptomatic individuals calls for structural abnormalities to be identified preferably through noninvasive studies (17). For diagnostic purposes, the 2010 TFC prescribe the use of transthoracic echocardiography (TTE), cardiac magnetic resonance (CMR), or RV angiography (6). Cardiac computed tomography (CT) is not part of the diagnostic TFC. This reflected low use of cine CT for ARVD/C because of high radiation dose and lack of use of the technology in multicenter clinical trials. However, a 2010 consensus document on the appropriate use of cardiac CT expressed the opinion that CT could be used for ARVD/C evaluation using more recently developed low radiation dose techniques (18). In this review, we will focus on noninvasive imaging modalities given their particular role in the setting of ARVD/C.

The utility of imaging techniques for ARVD/C is dependent on the technical aspects of the modality, potential to visualize the right side of the heart, experience of the technician, and expertise of the interpreter. Recognition of the strengths and weaknesses of each technique is crucial to facilitate optimal implementation of cardiac imaging in ARVD/C evaluation (Table 3). TTE often is the first-line imaging modality in a patient with suspected ARVD/C because of its widespread availability and low cost. TTE provides structural and functional information on all cardiac chambers, although visualization of the RV requires special emphasis and expertise. In addition, in patients with an implantable cardioverter-defibrillator (ICD), TTE may be used for serial evaluation to evaluate disease progression. CMR has high spatial resolution and a theoretically unlimited field of view, thereby allowing for detailed visualization of RV wall motion abnormalities. In addition, the 3-dimensional (3D) depiction of anatomy by CMR enables accurate measurement of RV volumes and function. Moreover, CMR with late gadolinium enhancement (LGE) offers the possibility to visualize intramyocardial fat and fibrosis, the pathologic hallmarks of ARVD/C. Cardiac CT, in particular multidetector computed tomography (MDCT), has excellent spatial resolution allowing for clear delineation of the ventricular endocardium. In addition, quantitative evaluation of ventricular volumes and function can be performed, and its capability to depict fatty tissue makes it an interesting option in the setting of ARVD/C. Until recently, the radiation dose of cine CT was an important drawback. However, our experience has shown that radiation exposure for cine CT may be reduced to clinically appropriate values (1 to 2 mSv) while maintaining good temporal and spatial resolution, reinforcing its potential as a diagnostic tool in ARVD/C.

TRANSTHORACIC ECHOCARDIOGRAPHY

A TTE examination is an ideal screening tool to assess RV size and function in patients with possible ARVD/C. TTE can be performed and interpreted easily and at low cost, and is widely accessible and portable. In addition, the technique is particularly useful in following affected individuals over time because of the ability to perform serial imaging in patients who have ICDs.

TTE FINDINGS

RV morphology—RV dilation is frequently observed in patients with ARVD/C (19,20). Data from the North American Multidisciplinary Study showed that an enlarged RV outflow tract was found in 100% of probands (19). In the 2010 TFC, a major criterion for ARVD/C is fulfilled when there is RV outflow tract dilation on the parasternal long-axis (≥32 mm) or short-axis (≥36 mm) view, along with localized akinesia, dyskinesia, or aneurysms (6) (Figures 1A and 1B). The presence of a wall motion abnormality with only mild dilation (≥29 to <32 mm for parasternal long axis and ≥32 to <36 mm for parasternal short axis) is a minor criterion (Table 1). These cutoff values were on the basis of data of 69 probands from the North American Multidisciplinary ARVD/C Study compared with 450 controls (6). It is important to recognize that for both major and minor criteria, a segmental wall motion abnormality also needs to be present (regional akinesia or dyskinesia).

RV dilation is not specific to ARVD/C. It has also been reported as a physiologic adaptation to high-intensity exercise (21). In addition, RV enlargement in ARVD/C has been associated

with an increased risk of sudden death and ventricular arrhythmias in athletes (4,22). Thus, the diagnosis of ARVD/C in highly trained athletes is challenging. A detailed medical and family history and careful application of the TFC exclusive of RV structure and function may help distinguish disease from normal adaptation to high-intensity exercise. In the future, the accuracy of TTE in this subset of individuals may be improved by the use of newer TTE parameters, such as tissue Doppler imaging (TDI) and speckle tracking for RV myocardial strain and strain rate (23).

In addition to RV enlargement, several morphologic abnormalities have been noted on TTE in individuals with ARVD/C (Figure 2). These include trabecular prominence and derangement and focal aneurysms or sacculations. Although trabecular hypertrophy/derangement has been described in published reports with increased frequency in ARVD/C (19), it is not specific to the disease, and thus is not part of the imaging diagnostic criteria. Trabecular prominence or derangement, assessed subjectively by the core laboratory echocardiographers, was defined in the North American registry as thickened, hypertrophied trabeculae that occupy a significant amount of the RV cavity at end diastole. It was the most frequently noted morphologic abnormality in the North American Multidisciplinary Study, observed in 54% of affected individuals and not in any matched controls (19).

RV function—Because of the asymmetric geometry of the RV and difficulty with visualization of the entire RV endocardium from standard TTE views in ARVD/C, estimation of RV volume and function by conventional 2-dimensional (2D) TTE is challenging. The RV fractional area change (FAC) from the apical 4-chamber view has been shown to be a useful correlate of global RV function (24) and is decreased in individuals with ARVD/C compared with controls (19). In the 2010 TFC, the presence of severe RV dysfunction (RV FAC ≤33%) combined with a localized wall motion abnormality constitutes a major diagnostic criterion, whereas mild RV dysfunction (RV FAC >33% to ≤40%) constitutes a minor criterion (Figures 1C and 1D). Unfortunately, there have been no large population studies describing normal values for RV FAC normalized for sex or body size. For the 2010 TFC, the optimal cutoff points for FAC were determined using data from the Multidisciplinary Study coupled with 450 controls. In the presence of regional wall motion abnormality, an FAC ≤33% has a sensitivity of 55% and a specificity of 95% for the diagnosis of ARVD/C (6).

TTE PROTOCOL

TTE for ARVD/C evaluation should be performed using current American Society of Echocardiography guidelines (25). Because the RV may be enlarged and therefore not completely visualized on standard imaging planes, additional off-axis images should be obtained to ensure that all parts of the RV free wall are well visualized. This is especially important given the patchy nature of this disease, to not miss localized RV aneurysms.

NEWER ECHOCARDIOGRAPHIC TECHNIQUES IN ARVD/C

Many new echocardiographic techniques have emerged to complement a standard 2D TTE examination in the setting of ARVD/C. A simple Doppler index of RV function, the RV myocardial performance index, is independent of geometric assumptions (26) and has been

applied in diseases affecting the RV, such as pulmonary hypertension (27). Preliminary data regarding the utility of this index in ARVD/C have demonstrated reduced RV myocardial performance index in ARVD/C probands, even when global RV function as assessed by FAC was normal (28). Another group found this to be a less-informative estimate of global RV dysfunction in ARVD/C (29). This index needs to be tested in larger populations to determine its diagnostic utility in individuals with suspected ARVD/C.

Use of intravenous TTE contrast has been described in populations with ARVD/C and can improve detection of subtle areas of regional dysfunction (30). Nemes et al. (31) recently suggested that abnormalities of RV perfusion can be detected in areas affected by fatty infiltration. Larger populations of patients with ARVD/C need to be studied to define the utility of contrast TTE in this disease.

Tricuspid annular plane systolic excursion measured with M-mode echocardiography or Doppler quantification of tricuspid valve annular motion using TDI can be used to estimate global RV function (20). These techniques are probably most useful when RV dysfunction is global or in those with advanced disease. Because annular motion may be preserved in early or subtle forms of ARVD/C, the utility of the tricuspid annular plane systolic excursion and TDI systolic velocity in screening suspected cases or mutation carriers who could have patchy or regional disease is limited.

3D TTE is an emerging tool that shows promise for accurate estimation of RV volumes and RV ejection fraction (32) (Figure 3, Online Video 1). Imaging of the entire RV volume from a single transducer position and single image acquisition is now possible using 3D TTE (33). RV volume calculated using this technique has been shown to have less variability than similar calculations by 2D TTE (34,35). RV ejection fractions calculated by 3D TTE have been shown to be decreased in ARVD/C compared with normal controls (36,37). 3D TTE parameters also have been shown to differentiate those with ARVD/C from unaffected relatives; however, variability was higher than noted in prior 3D TTE validation studies (32). At present, there are limitations in image quality with 3D TTE, as well as technical considerations of image acquisition, cropping, and measurement that require significant experience with the technique. Normal values and disease cutpoints are still being established; thus, the usefulness remains limited to specialized centers with expertise in the use and limitations of 3D TTE.

An important prerequisite of echocardiographic fulfillment of TFC is the presence of a segmental wall motion abnormality. However, it should be noted that there is significant variability in the morphology and motion of the normal RV. As such, qualitative evaluation of RV wall motion abnormalities is subjective and has been shown to have poor reproducibility (38). RV free wall myocardial velocity, strain, and strain rate by echocardiographic deformation imaging (by TDI or speckle tracking) are promising tools to quantify global and regional ventricular function. Systolic strain and systolic strain rate by TDI have been shown to be reduced in patients with ARVD/C compared with healthy controls (37,38), and use of this technique may be able to detect subtle early abnormalities in asymptomatic mutation carriers (39). One limitation of TDI is angle dependence, a requirement that the motion of the wall that is sampled is parallel to the ultrasound beam. As

the RV becomes significantly enlarged in more advanced ARVD/C, obtaining accurate and reproducible measures of RV peak systolic velocity, strain, and strain rate can be challenging. It is possible that assessment of RV strain and strain rate by speckle tracking might be more applicable in the ARVD/C population because it is not on the basis of Doppler and thus is not angle dependent. Although the findings described in these small research studies show promise, at present these measures are best performed at specialized centers by those experienced in the technique.

CMR IMAGING

CMR is well suited for comprehensive assessment of the RV. It enables good assessment of cardiac morphology and function while also allowing flow dynamic studies and tissue characterization. Important advantages of CMR are the multiplane capability and high spatial resolution, making it a highly sensitive tool for detecting subtle contraction abnormalities.

CMR FINDINGS IN ARVD/C

The interaction of CMR and ARVD/C began in 1987, when Casolo et al. (40) demonstrated intramyocardial fat deposits using conventional spin-echo imaging in a patient with advanced ARVD/C. In 1989, Wolf et al. (41) described “fat-like high signals” in the anterior RV and RV outflow tract using spin-echo sequence in 7 subjects with ARVD/C. Subsequently, Blake et al. (42) summarized prior CMR studies in a pictorial review advocating that “the essence of the diagnosis depends on the visualization of fat or extreme thinning in the infundibulum and the inferior or diaphragmatic free wall of the right ventricle.” Rather than ventricular thinning, our current emphasis is on regional wall motion abnormalities as the earlier and more reliable abnormalities identified by CMR (Figure 4).

CMR findings associated with ARVD/C include RV wall thinning, RV outflow tract enlargement, trabecular disarray, fibrofatty replacement, ventricular dilation, and global or regional systolic dysfunction (14,15,43). These abnormalities typically occur in predilection sites including the RV base and LV lateral wall (Central Illustration). Characteristic examples are shown in Figures 4 to 6. Given that fibrofatty change is the pathological hallmark of ARVD/C, many imagers are inclined to look for it to help support the diagnosis. In CMR studies, the prevalence of intra-myocardial hyperintense signal on T1-weighted spin-echo imaging indicative of fat ranged from 22% to 100% in different studies (44–48) (Figure 5). LGE CMR indicative of fibrosis was first described by Tandri et al. (49) in a cohort of 30 patients with ARVD/C. In subsequent studies, RV LGE was observed in up to 88% of patients (49–51), and left ventricular (LV) LGE was reported in up to 61% of cases (52,53) (Figure 6). In our opinion, the presence of LGE represents a late stage of ARVD/C; when LGE is present, multiple other findings of advanced disease are typically present (RV dilation and dysfunction).

Although the diagnostic Task Force recognized the presence of fat and LGE in many patients with ARVD/C, several limitations withheld their inclusion in the TFC. Intramyocardial fat occurs physiologically in older, obese patients and is not specific for ARVD/C in the absence of functional abnormalities (54,55). Intramyocardial fat was even

observed in 85% of autopsy cases dying of noncardiac causes (56). In comparison with fat infiltration, the detection of LGE indicative of fibrosis has technological and clinical limitations: Detection of fibrosis in the RV is non-specific and often hampered by the thin RV wall, which may be even more pronounced in ARVD/C (44).

CMR PROTOCOL FOR ARVD/C

The CMR protocol that we recommend for subjects with suspected ARVD/C recently has been described by te Riele et al. (15) (Table 4). In short, morphologic evaluation is preferably performed on fast spin-echo or turbo spin-echo imaging sequences. For cine imaging, we recommend the use of electrocardiogram-gated, steady-state free precession imaging at 1.5-T. Cine images should be obtained in the short-axis and horizontal long-axis views, whereas some sites prefer to also acquire a vertical long-axis view of the RV. With modern CMR scanners, the temporal resolution of cine images is typically approximately 40 ms. Quantitative analyses of the RV and LV are best performed on short-axis images. A phase-selective inversion recovery sequence is preferred for LGE imaging, because it is less dependent on the precise inversion time (57).

ROLE OF CMR IN ARVD/C DIAGNOSIS

Given the limitations of CMR evaluation of fat and fibrosis in ARVD/C, emphasis is currently placed on functional abnormalities. In the 2010 TFC, CMR criteria rely on the presence of both qualitative findings (RV regional akinesia, dyskinesia, or dyssynchronous contraction) and quantitative metrics (decreased RV ejection fraction or increased indexed RV end-diastolic volume) (Table 1). For derivation of quantitative cutoff values, RV dimensions and function from 462 normal MESA (Multi-Ethnic Study of Atherosclerosis) participants were compared with 44 probands in the North American Multidisciplinary ARVD/C Study (6). Cutoffs for major criteria (RV ejection fraction ≤40% or indexed RV end-diastolic volume ≥110 ml/m^2 for men and ≥100 ml/m^2 for women) were targeted to achieve approximately 95% specificity. Minor criteria (RV ejection fraction 40% to 45% or indexed RV end-diastolic volume 100 to 110 ml/m^2 for men and 90 to 100 ml/m^2 for women) had good sensitivity (79% to 89%), but a consequently lower specificity (58). It isimportant to recognize that for both major and minor criteria, a segmental wall motion abnormality also needs to be present (regional akinesia, dyskinesia, or dyssynchronous contraction).

A significant problem in the interpretation of CMR studies is the definition of normal versus subtle variants in RV contraction and morphology that may represent early disease versus normal variation. Even using quantitative parameters, there is considerable inter-reader variation (10% to 15%) in determination of RV volumes and ejection fraction. One approach may be for CMR laboratories to assess their own normal values in young adults and compare those values with published normal values to calibrate readings. For regional contraction abnormalities, no routine quantitative techniques are currently available.

ROLE OF CMR IN EARLY DIAGNOSIS AND RISK STRATIFICATION

CMR has been extensively used to characterize cardiac structural abnormalities in ARVD/C. Many of these studies predated the 2010 TFC and were performed in tertiary centers without

the availability of genetic testing. As such, almost all prior reports were populated by patients with severe phenotypes, and only a few reports have reported on structural changes in subjects with mild disease. A recent study among 80 mutation carriers across the spectrum of disease showed that wall motion abnormalities in the RV subtricuspid region were present in 94% of subjects with CMR structural involvement (13). Moreover, the RV subtricuspid region was abnormal in all patients with mild structural disease, suggesting that abnormalities in this region may be highly sensitive for early structural changes (Online Video 2). Rastegar et al. (59) extended these findings by demonstrating that fatty infiltration of the LV posterolateral wall can be observed in a substantial number of ARVD/C mutation carriers. In their study, this finding had no association with age or degree of RV structural abnormalities, challenging the concept that LV abnormalities occur only in late stages of ARVD/C.

An important, yet fairly new role of CMR lies in risk stratification for arrhythmic events. Previous studies have shown that severe RV dysfunction and LV involvement predict adverse outcome in ARVD/C (60,61). A recently published study among 69 ARVD/C mutation carriers showed that sustained arrhythmias during follow-up coincide with structural abnormalities on CMR (17). Moreover, no events were observed among subjects with a normal CMR evaluation during 6 years of follow-up. In addition, Deac et al. (62) demonstrated that CMR was an independent predictor of ventricular arrhythmia among 369 consecutive patients undergoing evaluation for ARVD/C. Large-scale studies from collaborative international registries are necessary to further enhance our understanding of arrhythmic risk stratification in ARVD/C.

NOVEL ADVANCES IN ARVD/C EVALUATION BY CMR

An important prerequisite of CMR fulfillment of TFC is the presence of regional wall motion abnormality. As such, fulfillment of CMR TFC is still “in the eye of the beholder” (58). Although a regional wall motion abnormality is necessary for ARVD/C TFC fulfillment, the normal RV has a nonuniform appearance, and distinguishing normal from abnormal may be a challenge particularly in the setting of RV volume overload or prominent tethering of the RV free wall by the moderator band. CMR tissue tracking, which has been used to quantify regional ventricular function in ARVD/C (63,64), may suggest one solution. We recently presented data on 106 subjects (39 with overt ARVD/C [genotype+, phenotype+], 37 with pre-clinical ARVD/C [genotype+, phenotype−], and 30 controls [genotype−, phenotype−]) who underwent CMR tissue tracking using steady-state free precession imaging (64). Mean segmental strain decreased in magnitude from control (−37.7 ± 11.2%) to pre-clinical (−32.2 ± 11.5%) to overt ARVD/C (−22.2 ± 11.9%), which constituted a highly significant trend. Differences between groups were most pronounced in the subtricuspid region, and peak strain in the 4-chamber plane was shown to be a better discriminator than peak strain in the axial plane, likely due to through-plane motion in the axial images. This approach will require improved standardization before routine use for ARVD/C is advocated.

LGE depends on differences in signal intensity between regions of scarring and adjacent normal myocardium. In subjects with diffuse fibrosis, these differences in signal intensity

are lacking, thus resulting in false-negative results. Over the last decade, measurement of myocardial T1 relaxation times (T1 mapping) with gadolinium-enhanced inversion recovery sequences has emerged as a novel approach for quantification of myocardial fibrosis (65). To the best of our knowledge, there have been no reports on T1 mapping in ARVD/C in published reports. A challenge of T1 mapping is that the technique has low spatial resolution, thus limiting application to the LV rather than the RV. New research pulse sequences have been developed to substantially improve spatial resolution. This suggests the future prospect of quantitative T1 mapping in ARVD/C. Although the technique is still in development, the strengths of T1 mapping as a noninvasive method for direct quantification of myocardial fibrosis have the potential to play an important role in ARVD/C evaluation and management.

COMPUTED TOMOGRAPHY

Similar to CMR, CT allows for tissue characterization, especially detection of fatty tissue, of the myocardium (Figure 7). Newer-generation CT scanners, including MDCT, provide superior spatial resolution compared with CMR, with comparable or superior temporal resolution. Quantitative evaluation of ventricular mass and RV and LV volume and function using MDCT has been validated against echocardiography (66) and CMR (67). In addition, the widespread availability of CT, reliable image quality, and fast acquisition at low costs make CT popular for cardiovascular evaluation.

CT FINDINGS IN ARVD/C

Dery et al. (68) were the first to describe a dilated hypokinetic RV with wall thinning by cine CT in a patient with ARVD/C in 1986. Two years later, Villa et al. (69) reported on RV enlargement, thinning of the RV myocardium, RV subepicardial fat, and RV hypokinesia in 7 patients with ARVD/C who underwent conventional CT. Biopsy confirmation of CT findings was provided by Sotozono et al. (70) in 1990, who also showed excellent biventricular anatomic visualization in an advanced ARVD/C case.

Kimura et al. (71) illustrated the utility of helical CT in ARVD/C evaluation by revealing abnormal RV structure and function among 32 patients who underwent single-row detector helical CT. Compared with conventional CT, electron-beam computed tomography (EBCT) received considerable attention because of its excellent temporal resolution with motionless cardiac and cross-sectional imaging. The use of EBCT in ARVD/C was first published in 1993. At that time, Hamada et al. (72) described an “enlarged RV, scalloped surface of the free wall, conspicuous trabeculations with low attenuation, and abundant epicardial adipose tissue” in 4 patients. The same study revealed regional dysfunction and depressed RV regional dysfunction on quantitative evaluation. Subsequently, Tada et al. (73) showed that EBCT findings have a high correlation with abnormalities on electrophysiologic study. The frequencies of epicardial fat, scalloping, low-attenuation trabeculae, and intramyocardial fat in this study were 86%, 79%, 71%, and 50%, respectively.

Although EBCT scanners are no longer generally available, similar cine and morphologic findings can be visualized using MDCT scanners. The relatively low spatial resolution and low signal-to-noise ratio of EBCT limited accurate morphological assessment (74). MDCT

allows for improved visualization of the myocardium with excellent spatial resolution and high signal-to-noise ratio, and thus could be more suitable for the assessment of biventricular tissue involvement (74). Before the first comprehensive study of MDCT in ARVD/C was performed (75), published data on MDCT in ARVD/C were limited to a handful of case reports (74,76–79). In 2007, Bomma et al. (75) confirmed the feasibility and diagnostic potential of MDCT in a series of 31 ARVD/C referrals, of whom 17 met diagnostic TFC. In addition, Nakajima et al. (80) showed that electrocardiogram-gated MDCT differentiated between ARVD/C and other causes of ventricular arrhythmia. Komatsu et al. (81) recently studied 16 patients with ARVD/C who underwent pre-procedural MDCT before epicardial ablation. The authors report good concordance between epicardial low voltage and fat on MDCT, with ablation targets clustering in the border of the fat region. This study reveals the potential of MDCT in the localization of an arrhythmic substrate and potential therapeutic applications in ARVD/C.

CT PROTOCOL FOR ARVD/C

Many patients with ARVD/C are young, and thus efforts must be made to reduce radiation dose otherwise associated with cine CT. The latest second- and third-generation CT scanners have enhanced reconstruction algorithms that allow reduced radiation exposure. In addition, the temporal resolution of scanners has dramatically improved over the past 5 to 10 years.

Patients undergoing cine CT likely require control of heart rate using antiarrhythmic medication. Multiple ectopic ventricular beats will result in high radiation dose and prolonged breath-holds. The optimum CT protocol will heavily depend on the technological sophistication of the CT equipment. However, several general conclusions can be made:

1. Calcium scoring and coronary artery imaging are generally not needed for ARVD/C patients. Reduction of these 2 components of the CT examination may reduce radiation dose by 3 to 10 mSv or more depending on the scanner generation.
2. Opacification of both the RV and the LV with iodinated contrast is necessary for optimal visualization of wall motion abnormalities. Thus, modification of the typical CT angiogram contrast injection protocol is needed (where contrast opacification of only the LV is usually desirable).
3. Temporal resolution of the CT image is worse than using CMR unless a segmented cardiac acquisition is used; segmented acquisitions (multiple heartbeats) in turn result in substantially increased radiation dose to the patient. Although a 320-slice CT scanner can produce an approximately 50 ms cine CT image in 3 heartbeats, an older generation 64-slice scanner may show markedly lower temporal resolution (100 to 150 ms) when used in a comparable multi-heartbeat mode.
4. Reconstruction oversampling of the time domain (cine) images is important to provide high-quality cine images. By using older 64-slice technology, we previously reconstructed 10 images during the cardiac cycle, or 1 image per 100 ms resolution (at 60 beats/min heart rate). On the other hand, 50 ms cine imaging is now available; 40 cine images per heart cycle can be reconstructed for optimal depiction of the cardiac cycle. Given the large number of CT images generated,

reconstructed slice thickness of 4 to 5 mm is sufficient for visualization and quantification of ventricular function.

CURRENT USE OF CT IN ARVD/C

Cardiac CT is not included in the diagnostic TFC and thus usually not part of the initial screening of patients with suspected ARVD/C. However, a possible use of CT lies in the evaluation of claustrophobic patients, assessment of subjects with frequent ventricular extrasystoles leading to severe arrhythmia artifacts on CMR, and serial evaluation of ICD carriers. Although CMR-compatible ICDs have become available, device artifacts degrade CMR quality, rendering the examination unusable. In addition, CT may be valuable for procedural planning of subjects undergoing ablation procedures (81). The latest third-generation MDCT scanners have the potential for 1 to 2 mSv cine CT images at acceptable temporal resolution (50 to 100 msV). We believe this modality will be increasingly used in the future for evaluation of patients with ARVD/C.

CONCLUSIONS

Noninvasive imaging plays an important role in ARVD/C evaluation. For diagnostic purposes, the 2010 TFC prescribe the use of TTE or CMR. Because of its low cost and widespread availability, conventional TTE is often used as a first-line imaging technique for ARVD/C. Although not included in the diagnostic criteria, previous studies have shown that echocardiographic deformation imaging using TDI or speckle tracking is a promising tool to diagnose early, subtle RV changes. CMR has 3D multiplane capability and high spatial resolution. CMR is uniquely suited for ARVD/C evaluation because it allows for both morphological and functional characterization, as well as evaluation of fibrofatty replacement, the pathologic hallmark of ARVD/C. Although not part of the diagnostic TFC, CT has excellent spatial resolution, reliable image quality, and fast acquisition at low costs. With the decreasing radiation dose and increasing familiarity of physicians with CT findings in ARVD/C, CT may play an important role both in the diagnosis and the follow-up of patients with ARVD/C. Studies comparing different imaging techniques would further our knowledge on the utility of each technique for ARVD/C evaluation.

Acknowledgments

This work was performed during Dr. te Riele's tenure as the Mark Josephson and Hein Wellens Research Fellow of the Heart Rhythm Society. Funding was received from the Dr. Francis P. Chiaramonte Private Foundation, St. Jude Medical, Inc., and Medtronic, Inc. The Johns Hopkins ARVD/C Program is supported by the Leyla Erkan Family Fund for ARVD research, the Dr. Satish, Rupal, and Robin Shah ARVD Fund at Johns Hopkins, the Bogle Foundation, the Healing Hearts Foundation, the Campanella family, the Patrick J. Harrison Family, the Peter French Memorial Foundation, and the Wilmerding Endowments.

ABBREVIATIONS AND ACRONYMS

ARVD/C	arrhythmogenic right ventricular dysplasia/cardiomyopathy
CMR	cardiac magnetic resonance
CT	computed tomography

EBCT	electron-beam computed tomography
FAC	fractional area change
ICD	implantable cardioverter-defibrillator
LGE	late gadolinium enhancement
LV	left ventricular
MDCT	multidetector computed tomography
RV	right ventricular
TDI	tissue Doppler imaging
TFC	Task Force Criteria
3D	3-dimensional
TTE	transthoracic echocardiography
2D	2-dimensional

References

1. Marcus FI, Fontaine GH, Guiraudon G, et al. Right ventricular dysplasia: a report of 24 adult cases. Circulation. 1982; 65:384–98. [PubMed: 7053899]
2. Murray B. Arrhythmogenic right ventricular dysplasia/cardiomyopathy (ARVD/C): a review of molecular and clinical literature. J Genet Couns. 2012; 21:494–504. [PubMed: 22426942]
3. Corrado D, Thiene G, Nava A, Rossi L, Pennelli N. Sudden death in young competitive athletes: clinicopathologic correlations in 22 cases. Am J Med. 1990; 89:588–96. [PubMed: 2239978]
4. Thiene G, Nava A, Corrado D, Rossi L, Pennelli N. Right ventricular cardiomyopathy and sudden death in young people. N Engl J Med. 1988; 318:129–33. [PubMed: 3336399]
5. Dalal D, Nasir K, Bomma C, et al. Arrhythmogenic right ventricular dysplasia: a United States experience. Circulation. 2005; 112:3823–32. [PubMed: 16344387]
6. Marcus FI, McKenna WJ, Sherrill D, et al. Diagnosis of arrhythmogenic right ventricular cardiomyopathy/dysplasia: proposed modification of the task force criteria. Circulation. 2010; 121:1533–41. [PubMed: 20172911]
7. McKoy G, Protonotarios N, Crosby A, et al. Identification of a deletion in plakoglobin in arrhythmogenic right ventricular cardiomyopathy with palmoplantar keratoderma and woolly hair (Naxos disease). Lancet. 2000; 355:2119–24. [PubMed: 10902626]
8. Rampazzo A, Nava A, Malacrida S, et al. Mutation in human desmoplakin domain binding to plakoglobin causes a dominant form of arrhythmogenic right ventricular cardiomyopathy. Am J Hum Genet. 2002; 71:1200–6. [PubMed: 12373648]
9. Pilichou K, Nava A, Basso C, et al. Mutations in desmoglein-2 gene are associated with arrhythmogenic right ventricular cardiomyopathy. Circulation. 2006; 113:1171–9. [PubMed: 16505173]
10. Gerull B, Heuser A, Wichter T, et al. Mutations in the desmosomal protein plakophilin-2 are common in arrhythmogenic right ventricular cardiomyopathy. Nat Genet. 2004; 36:1162–4. [PubMed: 15489853]
11. Syrris P, Ward D, Evans A, et al. Arrhythmogenic right ventricular dysplasia/cardiomyopathy associated with mutations in the desmosomal gene desmocollin-2. Am J Hum Genet. 2006; 79:978–84. [PubMed: 17033975]
12. Delmar M, McKenna WJ. The cardiac desmosome and arrhythmogenic cardiomyopathies: from gene to disease. Circ Res. 2010; 107:700–14. [PubMed: 20847325]

13. te Riele AS, James CA, Philips B, et al. Mutation-positive arrhythmogenic right ventricular dysplasia/cardiomyopathy: the triangle of dysplasia displaced. J Cardiovasc Electrophysiol. 2013; 24:1311–20. [PubMed: 23889974]
14. Tandri H, Bomma C, Calkins H, Bluemke DA. Magnetic resonance and computed tomography imaging of arrhythmogenic right ventricular dysplasia. J Magn Reson Imaging. 2004; 19:848–58. [PubMed: 15170788]
15. te Riele AS, Tandri H, Bluemke DA. Arrhythmogenic right ventricular cardiomyopathy: cardiovascular magnetic resonance update. J Cardiovasc Magn Reson. 2014; 16:50. [PubMed: 25191878]
16. Rastegar N, Burt JR, Corona-Villalobos CP, et al. Cardiac MR findings and potential diagnostic pitfalls in patients evaluated for arrhythmogenic right ventricular cardiomyopathy. Radiographics. 2014; 34:1553–70. [PubMed: 25310417]
17. te Riele AS, Bhonsale A, James CA, et al. Incremental value of cardiac magnetic resonance imaging in arrhythmic risk stratification of arrhythmogenic right ventricular dysplasia/cardiomyopathy-associated desmosomal mutation carriers. J Am Coll Cardiol. 2013; 62:1761–9. [PubMed: 23810894]
18. Taylor AJ, Cerqueira M, Hodgson JM, et al. ACCF/SCCT/ACR/AHA/ASE/ASNC/NASCI/SCAI/SCMR 2010 appropriate use criteria for cardiac computed tomography. A report of the American College of Cardiology Foundation Appropriate Use Criteria Task Force, the Society of Cardiovascular Computed Tomography, the American College of Radiology, the American Heart Association, the American Society of Echocardiography, the American Society of Nuclear Cardiology, the North American Society for Cardiovascular Imaging, the Society for Cardiovascular Angiography and Interventions, and the Society for Cardiovascular Magnetic Resonance. J Am Coll Cardiol. 2010; 56:1864–94. [PubMed: 21087721]
19. Yoerger DM, Marcus F, Sherrill D, et al. Echocardiographic findings in patients meeting task force criteria for arrhythmogenic right ventricular dysplasia: new insights from the multidisciplinary study of right ventricular dysplasia. J Am Coll Cardiol. 2005; 45:860–5. [PubMed: 15766820]
20. Lindstrom L, Wilkenshoff UM, Larsson H, Wranne B. Echocardiographic assessment of arrhythmogenic right ventricular cardiomyopathy. Heart. 2001; 86:31–8. [PubMed: 11410558]
21. La Gerche A, Claessen G, Van de Bruaene A, et al. Cardiac MRI: a new gold standard for ventricular volume quantification during high-intensity exercise. Circ Cardiovasc Imaging. 2013; 6:329–38. [PubMed: 23258478]
22. Corrado D, Fontaine G, Marcus FI, et al. Arrhythmogenic right ventricular dysplasia/cardiomyopathy: need for an international registry. Study Group on Arrhythmogenic Right Ventricular Dysplasia/Cardiomyopathy of the Working Groups on Myocardial and Pericardial Disease and Arrhythmias of the European Society of Cardiology and of the Scientific Council on Cardiomyopathies of the World Heart Federation. Circulation. 2000; 101:E101–6. [PubMed: 10725299]
23. La Gerche A, Burns AT, D'Hooge J, Macisaac AI, Heidbuchel H, Prior DL. Exercise strain rate imaging demonstrates normal right ventricular contractile reserve and clarifies ambiguous resting measures in endurance athletes. J Am Soc Echocardiogr. 2012; 25:253–62. e1. [PubMed: 22192334]
24. Lang RM, Bierig M, Devereux RB, et al. Recommendations for chamber quantification: a report from the American Society of Echocardiography's Guidelines and Standards Committee and the Chamber Quantification Writing Group, developed in conjunction with the European Association of Echocardiography, a branch of the European Society of Cardiology. J Am Soc Echocardiogr. 2005; 18:1440–63. [PubMed: 16376782]
25. Rudski LG, Lai WW, Afilalo J, et al. Guidelines for the echocardiographic assessment of the right heart in adults: a report from the American Society of Echocardiography endorsed by the European Association of Echocardiography, a registered branch of the European Society of Cardiology, and the Canadian Society of Echocardiography. J Am Soc Echocardiogr. 2010; 23:685–713. quiz 786–8. [PubMed: 20620859]
26. Tei C, Dujardin KS, Hodge DO, et al. Doppler echocardiographic index for assessment of global right ventricular function. J Am Soc Echocardiogr. 1996; 9:838–47. [PubMed: 8943444]

27. Sebbag I, Rudski LG, Therrien J, Hirsch A, Langleben D. Effect of chronic infusion of epoprostenol on echocardiographic right ventricular myocardial performance index and its relation to clinical outcome in patients with primary pulmonary hypertension. Am J Cardiol. 2001; 88:1060–3. [PubMed: 11704014]
28. Yoerger DM, Marcus F, Sherrill D, et al. Right ventricular myocardial performance index in pro-bands from the multicenter study of arrhythmogenic right ventricular dysplasia (abstr). J Am Coll Cardiol. 2005; 45:147A.
29. Wang J, Prakasa K, Bomma C, et al. Comparison of novel echocardiographic parameters of right ventricular function with ejection fraction by cardiac magnetic resonance. J Am Soc Echocardiogr. 2007; 20:1058–64. [PubMed: 17555927]
30. Lopez-Fernandez T, Garcia-Fernandez MA, Perez David E, Moreno Yanguela M. Usefulness of contrast echocardiography in arrhythmogenic right ventricular dysplasia. J Am Soc Echocardiogr. 2004; 17:391–3. [PubMed: 15044876]
31. Nemes A, Vletter WB, Scholten MF, ten Cate FJ. Contrast echocardiography for perfusion in right ventricular cardiomyopathy. Eur J Echocardiogr. 2005; 6:470–2. [PubMed: 16293534]
32. Prakasa KR, Dalal D, Wang J, et al. Feasibility and variability of three dimensional echocardiography in arrhythmogenic right ventricular dysplasia/cardiomyopathy. Am J Cardiol. 2006; 97:703–9. [PubMed: 16490442]
33. Picard, MH. Three dimensional echocardiography. In: Otto, CM., editor. The Practice of Clinical Echocardiography. Philadelphia, PA: Elsevier; 2007. p. 86
34. Jiang L, Vazquez de Prada JA, Handschumacher MD, et al. Three-dimensional echocardiography: in vivo validation for right ventricular free wall mass as an index of hypertrophy. J Am Coll Cardiol. 1994; 23:1715–22. [PubMed: 8195537]
35. Jiang L, Siu SC, Handschumacher MD, et al. Three-dimensional echocardiography. In vivo validation for right ventricular volume and function. Circulation. 1994; 89:2342–50. [PubMed: 8181160]
36. Kjaergaard J, Hastrup Svendsen J, Sogaard P, et al. Advanced quantitative echocardiography in arrhythmogenic right ventricular cardiomyopathy. J Am Soc Echocardiogr. 2007; 20:27–35. [PubMed: 17218199]
37. Vitarelli A, Cortes Morichetti M, Capotosto L, et al. Utility of strain echocardiography at rest and after stress testing in arrhythmogenic right ventricular dysplasia. Am J Cardiol. 2013; 111:1344–50. [PubMed: 23411103]
38. Teske AJ, Cox MG, De Boeck BW, Doevendans PA, Hauer RN, Cramer MJ. Echocardiographic tissue deformation imaging quantifies abnormal regional right ventricular function in arrhythmogenic right ventricular dysplasia/cardiomyopathy. J Am Soc Echocardiogr. 2009; 22:920–7. [PubMed: 19553080]
39. Teske AJ, Cox MG, te Riele AS, et al. Early detection of regional functional abnormalities in asymptomatic ARVD/C gene carriers. J Am Soc Echocardiogr. 2012; 25:997–1006. [PubMed: 22727198]
40. Casolo GC, Poggesi L, Boddi M, et al. ECG-gated magnetic resonance imaging in right ventricular dysplasia. Am Heart J. 1987; 113:1245–8. [PubMed: 3578022]
41. Wolf JE, Rose-Pittet L, Page E, et al. Detection of parietal lesions using magnetic resonance imaging in arrhythmogenic dysplasia of the right ventricle. Arch Mal Coeur Vaiss. 1989; 82:1711–7. [PubMed: 2531998]
42. Blake LM, Scheinman MM, Higgins CB. MR features of arrhythmogenic right ventricular dysplasia. AJR Am J Roentgenol. 1994; 162:809–12. [PubMed: 8140995]
43. Jain A, Tandri H, Calkins H, Bluemke DA. Role of cardiovascular magnetic resonance imaging in arrhythmogenic right ventricular dysplasia. J Cardiovasc Magn Reson. 2008; 10:32. [PubMed: 18570661]
44. Tandri H, Calkins H, Nasir K, et al. Magnetic resonance imaging findings in patients meeting task force criteria for arrhythmogenic right ventricular dysplasia. J Cardiovasc Electrophysiol. 2003; 14:476–82. [PubMed: 12776863]
45. Midiri M, Finazzo M, Brancato M, et al. Arrhythmogenic right ventricular dysplasia: MR features. Eur Radiol. 1997; 7:307–12. [PubMed: 9087346]

46. Auffermann W, Wichter T, Breithardt G, Joachimsen K, Peters PE. Arrhythmogenic right ventricular disease: MR imaging vs angiography. AJR Am J Roentgenol. 1993; 161:549–55. [PubMed: 8352102]
47. Ricci C, Longo R, Pagnan L, et al. Magnetic resonance imaging in right ventricular dysplasia. Am J Cardiol. 1992; 70:1589–95. [PubMed: 1466328]
48. Molinari G, Sardanelli F, Gaita F, et al. Right ventricular dysplasia as a generalized cardiomyopathy? findings on magnetic resonance imaging. Eur Heart J. 1995; 16:1619–24. [PubMed: 8881856]
49. Tandri H, Saranathan M, Rodriguez ER, et al. Noninvasive detection of myocardial fibrosis in arrhythmogenic right ventricular cardiomyopathy using delayed-enhancement magnetic resonance imaging. J Am Coll Cardiol. 2005; 45:98–103. [PubMed: 15629382]
50. Pfluger HB, Phrommintikul A, Mariani JA, Cherayath JG, Taylor AJ. Utility of myocardial fibrosis and fatty infiltration detected by cardiac magnetic resonance imaging in the diagnosis of arrhythmogenic right ventricular dysplasia–a single centre experience. Heart Lung Circ. 2008; 17:478–83. [PubMed: 18538631]
51. Hunold P, Wieneke H, Bruder O, et al. Late enhancement: a new feature in MRI of arrhythmogenic right ventricular cardiomyopathy? J Cardiovasc Magn Reson. 2005; 7:649–55. [PubMed: 16136854]
52. Marra MP, Leoni L, Bauce B, et al. Imaging study of ventricular scar in arrhythmogenic right ventricular cardiomyopathy: comparison of 3D standard electroanatomical voltage mapping and contrast-enhanced cardiac magnetic resonance. Circ Arrhythm Electrophysiol. 2012; 5:91–100. [PubMed: 22139887]
53. Santangeli P, Pieroni M, Dello Russo A, et al. Noninvasive diagnosis of electroanatomic abnormalities in arrhythmogenic right ventricular cardiomyopathy. Circ Arrhythm Electrophysiol. 2010; 3:632–8. [PubMed: 20937720]
54. Basso C, Thiene G. Adipositas cordis, fatty infiltration of the right ventricle, and arrhythmogenic right ventricular cardiomyopathy. Just a matter of fat? Cardiovasc Pathol. 2005; 14:37–41. [PubMed: 15710290]
55. Tandri H, Castillo E, Ferrari VA, et al. Magnetic resonance imaging of arrhythmogenic right ventricular dysplasia: sensitivity, specificity, and observer variability of fat detection versus functional analysis of the right ventricle. J Am Coll Cardiol. 2006; 48:2277–84. [PubMed: 17161260]
56. Tansey DK, Aly Z, Sheppard MN. Fat in the right ventricle of the normal heart. Histopathology. 2005; 46:98–104. [PubMed: 15656892]
57. Plaisier AS, Burgmans MC, Vonken EP, et al. Image quality assessment of the right ventricle with three different delayed enhancement sequences in patients suspected of ARVC/D. Int J Cardiovasc Imaging. 2012; 28:595–601. [PubMed: 21503703]
58. Bluemke DA. ARVC: imaging diagnosis is still in the eye of the beholder. J Am Coll Cardiol Img. 2011; 4:288–91.
59. Rastegar N, Zimmerman SL, te Riele AS, et al. Spectrum of biventricular involvement on CMR among carriers of ARVD/C-associated mutations. J Am Coll Cardiol Img. 2014 Nov 12. E-pub ahead of print.
60. Corrado D, Leoni L, Link MS, et al. Implantable cardioverter-defibrillator therapy for prevention of sudden death in patients with arrhythmogenic right ventricular cardiomyopathy/dysplasia. Circulation. 2003; 108:3084–91. [PubMed: 14638546]
61. Saguner AM, Vecchiati A, Baldinger SH, et al. Different prognostic value of functional right ventricular parameters in arrhythmogenic right ventricular cardiomyopathy/dysplasia. Circ Cardiovasc Imaging. 2014; 7:230–9. [PubMed: 24515411]
62. Deac M, Alpendurada F, Fanaie F, et al. Prognostic value of cardiovascular magnetic resonance in patients with suspected arrhythmogenic right ventricular cardiomyopathy. Int J Cardiol. 2013; 168:3514–21. [PubMed: 23701935]
63. Heermann P, Hedderich DM, Paul M, et al. Biventricular myocardial strain analysis in patients with arrhythmogenic right ventricular cardiomyopathy (ARVC) using cardiovascular magnetic resonance feature tracking. J Cardiovasc Magn Reson. 2014; 16:75. [PubMed: 25315082]

64. Vigneault DM, te Riele AS, James CA, et al. Abnormal right ventricular strain by cardiac magnetic resonance in preclinical arrhythmogenic right ventricular cardiomyopathy (abstr). Circulation. 2014; 130:A16584.

65. Burt JR, Zimmerman SL, Kamel IR, Halushka M, Bluemke DA. Myocardial t1 mapping: techniques and potential applications. Radiographics. 2014; 34:377–95. [PubMed: 24617686]

66. Dogan H, Kroft LJ, Bax JJ, et al. MDCT assessment of right ventricular systolic function. AJR Am J Roentgenol. 2006; 186:S366–70. [PubMed: 16714610]

67. Raman SV, Cook SC, McCarthy B, Ferketich AK. Usefulness of multidetector row computed tomography to quantify right ventricular size and function in adults with either tetralogy of Fallot or transposition of the great arteries. Am J Cardiol. 2005; 95:683–6. [PubMed: 15721122]

68. Dery R, Lipton MJ, Garrett JS, Abbott J, Higgins CB, Schienman MM. Cine-computed tomography of arrhythmogenic right ventricular dysplasia. J Comput Assist Tomogr. 1986; 10:120–3. [PubMed: 3944294]

69. Villa A, Di Guglielmo L, Salerno J, Klercy C, Kluzer A, Codega S. Arrhythmogenic dysplasia of the right ventricle. Evaluation of 7 cases using computerized tomography. Radiol Med. 1988; 75:28–35. [PubMed: 2964679]

70. Sotozono K, Imahara S, Masuda H, et al. Detection of fatty tissue in the myocardium by using computerized tomography in a patient with arrhythmogenic right ventricular dysplasia. Heart Vessels Suppl. 1990; 5:59–61. [PubMed: 2093715]

71. Kimura F, Sakai F, Sakomura Y, et al. Helical CT features of arrhythmogenic right ventricular cardiomyopathy. Radiographics. 2002; 22:1111–24. [PubMed: 12235341]

72. Hamada S, Takamiya M, Ohe T, Ueda H. Arrhythmogenic right ventricular dysplasia: evaluation with electron-beam CT. Radiology. 1993; 187:723–7. [PubMed: 8497621]

73. Tada H, Shimizu W, Ohe T, et al. Usefulness of electron-beam computed tomography in arrhythmogenic right ventricular dysplasia. Relationship to electrophysiological abnormalities and left ventricular involvement. Circulation. 1996; 94:437–44. [PubMed: 8759086]

74. Matsuo S, Sato Y, Nakae I, et al. Left ventricular involvement in arrhythmogenic right ventricular cardiomyopathy demonstrated by multidetector-row computed tomography. Int J Cardiol. 2007; 115:e129–31. [PubMed: 17166609]

75. Bomma C, Dalal D, Tandri H, et al. Evolving role of multidetector computed tomography in evaluation of arrhythmogenic right ventricular dysplasia/cardiomyopathy. Am J Cardiol. 2007; 100:99–105. [PubMed: 17599449]

76. Nishiyama K, Tadamura E, Kanao E, et al. Arrhythmogenic right ventricular dysplasia/ cardiomyopathy assessed with 64-slice computed tomography. Eur Heart J. 2006; 27:2666. [PubMed: 16717076]

77. Wu YW, Tadamura E, Kanao S, et al. Structural and functional assessment of arrhythmogenic right ventricular dysplasia/cardiomyopathy by multi-slice computed tomography: comparison with cardiovascular magnetic resonance. Int J Cardiol. 2007; 115:e118–21. [PubMed: 17101183]

78. Omichi C, Sugiyabu Y, Kakizawa Y, Endo M. Three-dimensional image of arrhythmogenic right ventricular dysplasia/cardiomyopathy reconstructed with 64-multislice computed tomography. Heart Rhythm. 2008; 5:1631–2. [PubMed: 18599362]

79. Soh EK, Villines TC, Feuerstein IM. Sixty-four-multislice computed tomography in a patient with arrhythmogenic right ventricular dysplasia. J Cardiovasc Comput Tomogr. 2008; 2:191–2. [PubMed: 19083946]

80. Nakajima T, Kimura F, Kajimoto K, Kasanuki H, Hagiwara N. Utility of ECG-gated MDCT to differentiate patients with ARVC/D from patients with ventricular tachyarrhythmias. J Cardiovasc Comput Tomogr. 2013; 7:223–33. [PubMed: 23992839]

81. Komatsu Y, Jadidi A, Sacher F, et al. Relationship between MDCT-imaged myocardial fat and ventricular tachycardia substrate in arrhythmogenic right ventricular cardiomyopathy. J Am Heart Assoc. 2014; 3(4) http://dx.doi.org/10.1161/JAHA.114.000935.

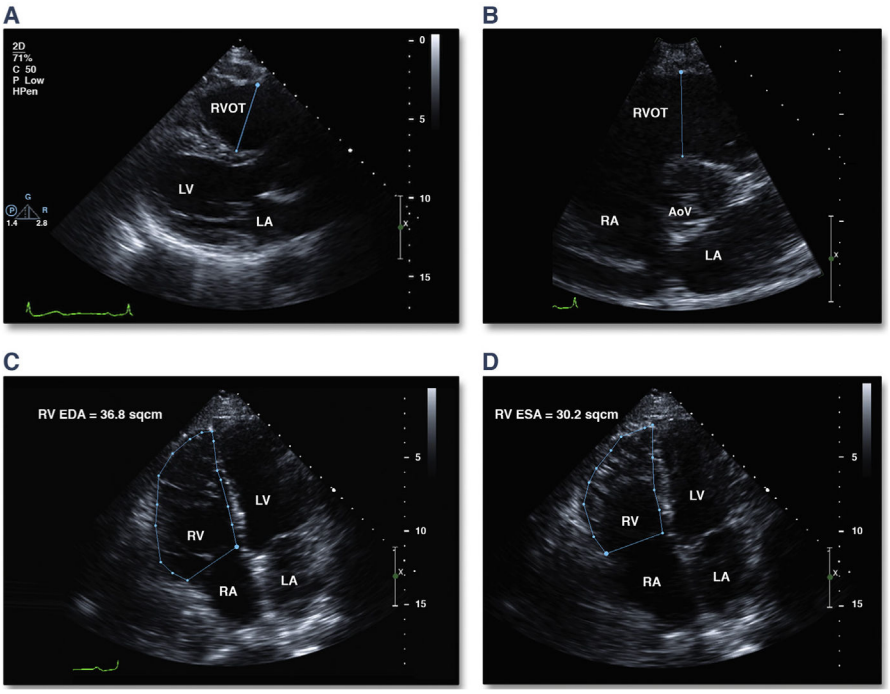

FIGURE 1. Quantitative Measures of RV Dilation and Function on Conventional TTE

(A) RVOT measurement from the parasternal long-axis view. **(B)** RVOT measurement from the parasternal short-axis view. RV FAC measurements should be taken from the apical 4-chamber view at end diastole **(C)** and end systole **(D)**. FAC is calculated from the formula: FAC = ([RV EDA − RV ESA]/RV EDA) · 100). AoV = aortic valve; EDA = end-diastolic area; ESA = end-systolic area; FAC = fractional area change; LA = left atrium; LV = left ventricle; RA = right atrium; RV = right ventricle; RVOT = right ventricular outflow tract; TTE = transthoracic echocardiography.

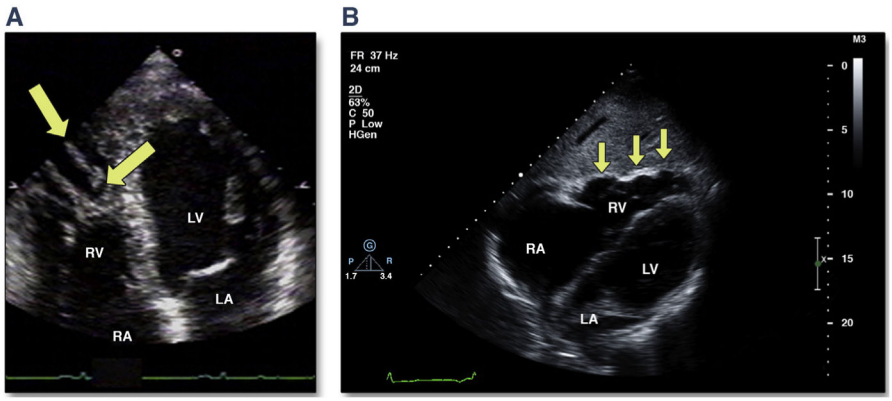

FIGURE 2. Morphologic Abnormalities in ARVD/C by TTE

(A) Apical 4-chamber view showing a highly trabeculated RV with trabecular derangement **(arrows). (B)** Subcostal long-axis view showing localized RV free wall aneurysms **(arrows)**. ARVD/C = arrhythmogenic right ventricular dysplasia/cardiomyopathy; other abbreviations as in Figure 1.

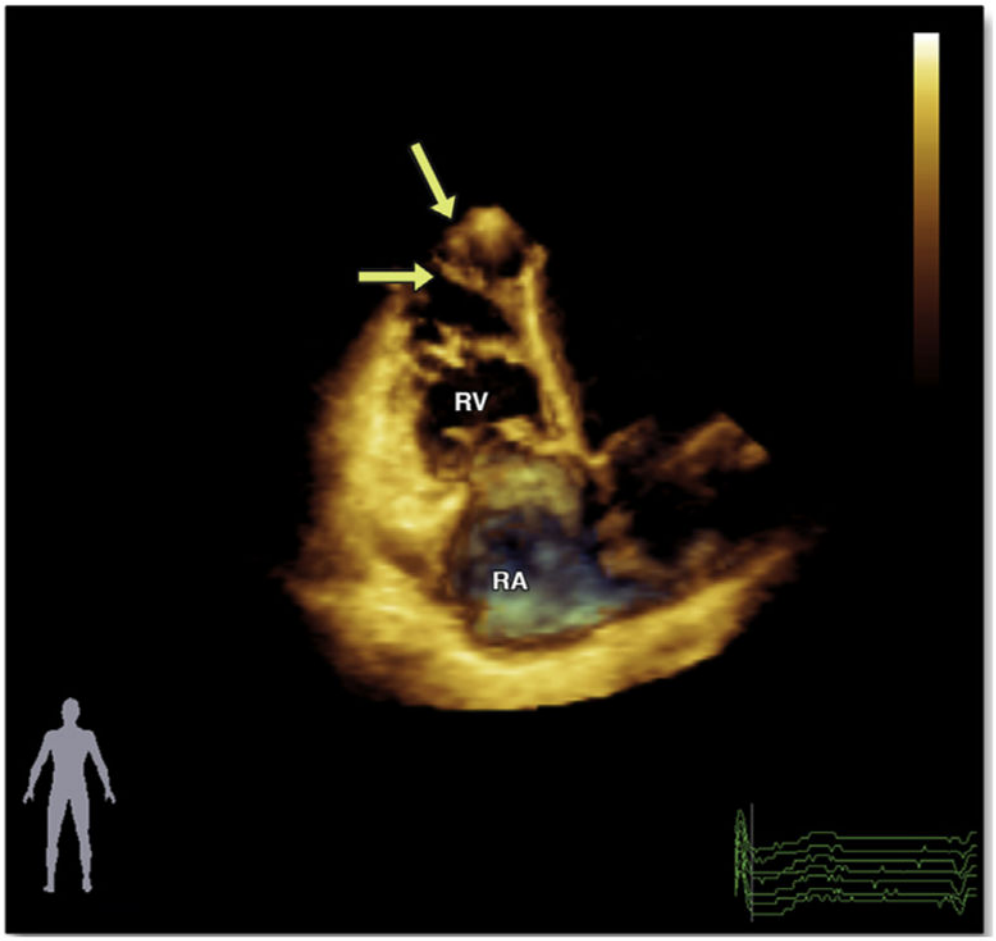

FIGURE 3. Three-Dimensional Echocardiography in the Apical View in a Patient With ARVD/C

Please note an enlarged globally hypokinetic RV. The apex is significantly dilated, and there is trabecular prominence **(arrows)**. The accompanying video file (Online Video 1) demonstrates the severe global RV dysfunction with akinesia of the RV apex and prominent trabeculae. Abbreviations as in Figures 1 and 2.

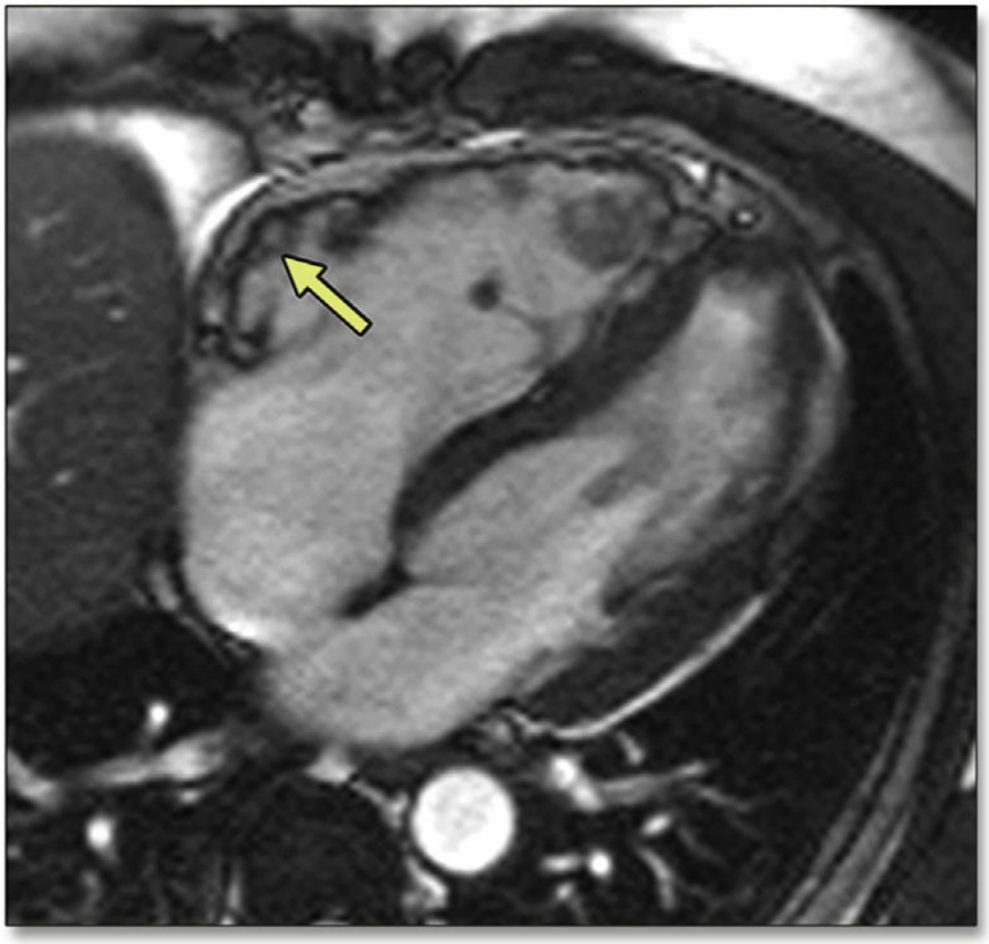

FIGURE 4. Four-Chamber Bright Blood Image by CMR of a 50-Year-Old Man With ARVD/C
Note the dilated RV with diastolic bulging in the subtricuspid region **(arrow)**. Please see Online Video 2. CMR = cardiac magnetic resonance; other abbreviations as in Figures 1 and 2.

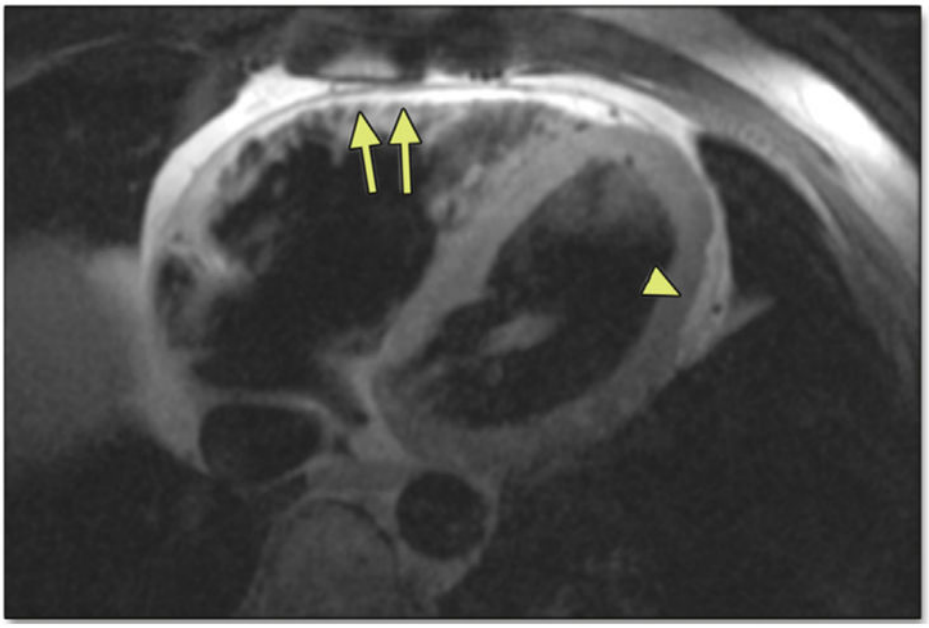

FIGURE 5. Horizontal Long-Axis Dark Blood Image by CMR in a 46-Year-Old Man With ARVD/C

Note the high-intensity signal suggestive of fat in the RV free wall extending as “fingers” into the myocardium **(arrows)**. Also note subepicardial fat and myocardial wall thinning in the LV posterolateral wall **(arrowhead)**. Abbreviations as in Figures 1, 2, and 4.

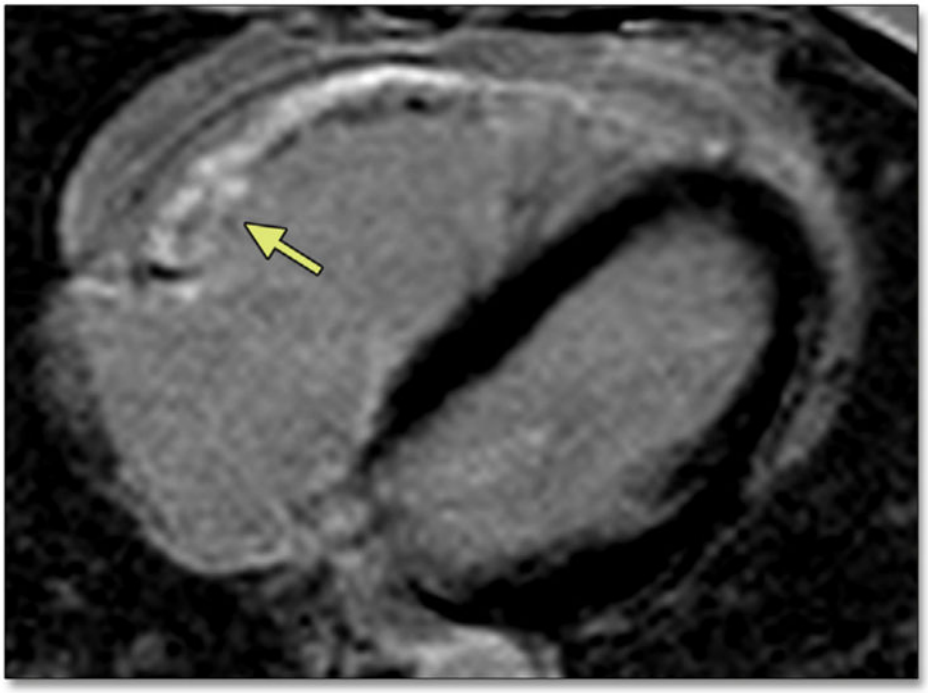

FIGURE 6. Phase-Sensitive Inversion Recovery Image After Administration of a Gadolinium Chelate by CMR in a 47-Year-Old Woman With ARVD/C

There is delayed enhancement in the subtricuspid region, suggestive of fibrosis **(arrow)**. Abbreviations as in Figures 2 and 4.

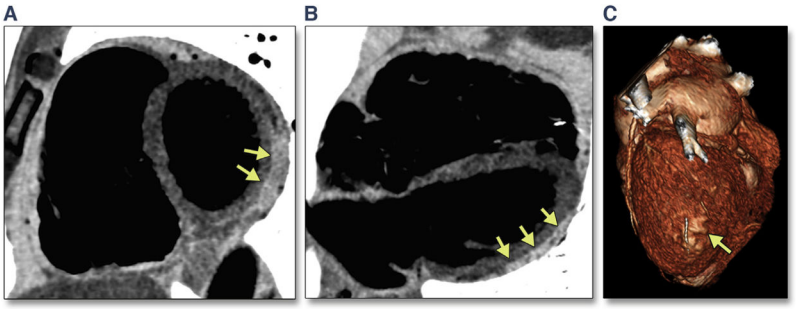

FIGURE 7. Identification of Fatty Tissue Using CT With Inverted Gray Scale in a 43-Year-Old Man With ARVD/C

(A) Short-axis and **(B)** horizontal long-axis CT images revealing hyperintense signal indicative of fat in the LV posterolateral wall **(arrows). (C)** Reconstructed 3D image showing subepicardial fat in the LV posterolateral wall in the same patient **(arrow)**. CT = computed tomography; 3D = 3-dimensional; other abbreviations as in Figures 1 and 2.

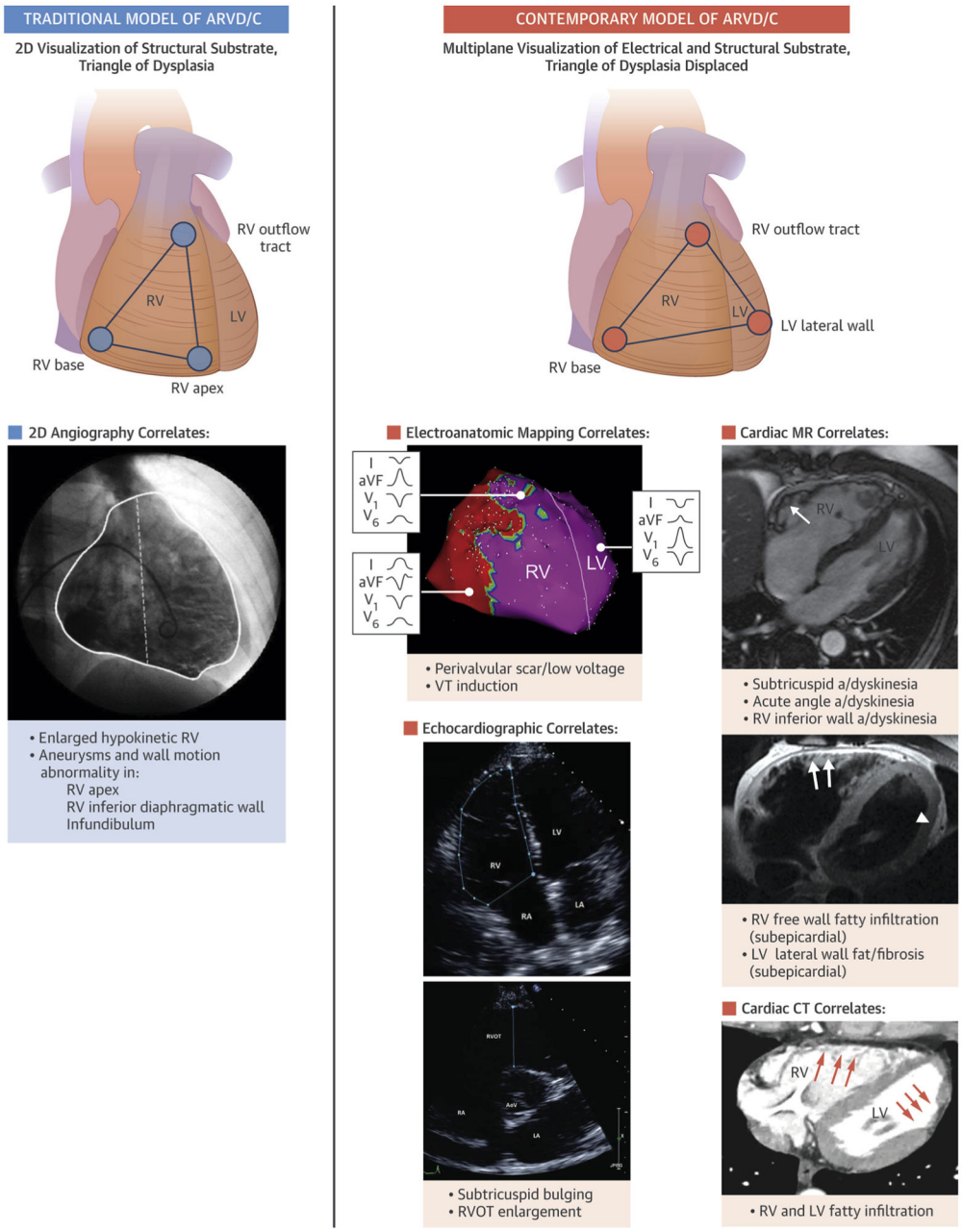

CENTRAL ILLUSTRATION. Traditional and Contemporary Model of Myocardial Involvement by ARVD/C

(Left) The concept of the “triangle of dysplasia” recognized primarily right ventricular (RV) disease involvement as visualized by angiography (RV base, outflow tract, and apex). **(Right)** Contemporary 3-dimensional imaging and electroanatomic mapping frequently reveals biventricular involvement by ARVD/C, involving the RV base, outflow tract, and lateral wall of the left ventricle. Two-dimensional angiography image in traditional ARVD/C model reproduced with kind permission from Springer Science and Business Media (original manuscript Indik et al., Int J Cardiovasc Img 2012;28:995–1001).

TABLE 1

Revised 2010 TFC for ARVD/C*

1 Global or Regional Dysfunction and Structural Alterations

Major

2D echocardiographic criteria

Regional RV akinesia, dyskinesia, or aneurysm and 1 of the following measured at end diastole:

- PLAX RVOT ≥32 mm (PLAX/BSA ≥19 mm/m^2),
- PSAX RVOT ≥36 mm (PSAX/BSA ≥21 mm/m^2), or
- FAC ≤33%

CMR criteria

Regional RV akinesia or dyskinesia or dyssynchronous RV contraction and 1 of the following:

- RV EDV/BSA ≥110 ml/m^2 (male) or ≥100 ml/m^2 (female)
- RV ejection fraction ≤40%

RV angiography criteria

Regional RV akinesia, dyskinesia, or aneurysm

Minor

2D echocardiographic criteria

Regional RV akinesia or dyskinesia and 1 of the following measured at end diastole:

- PLAX RVOT ≥29 to <32 mm (PLAX/BSA ≥16–<19 mm/m^2), or
- PSAX RVOT ≥32 to <36 mm (PSAX/BSA ≥18–<21 mm/m^2), or
- FAC >33% ≤40%

CMR criteria

Regional RV akinesia or dyskinesia or dyssynchronous RV contraction and 1 of the following:

- RV EDV/BSA ≥100–<110 ml/m^2 (male) or ≥90–<100 ml/m^2 (female)
- RV ejection fraction >40–≤45%

2 Tissue Characterization of Wall

Major

Residual myocytes <60% by morphometric analysis (or <50% if estimated), with fibrous replacement of the RV free wall myocardium in ≥1 sample, with or without fatty replacement of tissue on endomyocardial biopsy

Minor

Residual myocytes 60%–75% by morphometric analysis (or 50%–65% if estimated), with fibrous replacement of the RV free wall myocardium in ≥1 sample with or without fatty replacement of tissue on endomyocardial biopsy

3 Repolarization Abnormalities

Major

Inverted T waves in right precordial leads (V_1, V_2, and V_3) or beyond in individuals >14 yrs of age (in the absence of complete RBBB)

Minor

Inverted T waves in V_1 and V_2 in individuals >14 yrs of age (in the absence of complete RBBB) or in V_4, V_5, and V_6

Inverted T waves in leads V_1, V_2, V_3, and V_4 in individuals >14 yrs of age in the presence of a complete RBBB

4 Depolarization/Conduction Abnormalities

Major

Epsilon wave (reproducible low-amplitude signals between end of QRS complex to onset of T-wave) in the right precordial leads (V_1–V_3)

Minor

Late potentials by SAECG in ≥1 of 3 parameters in the absence of a QRSd of ≥110 ms on standard ECG:

- Filtered QRS duration (≥114 ms)
- Duration of terminal QRS <40 μV ≥38 ms
- Root mean square voltage of terminal 40 ms ≤20 μV

Terminal activation duration of ≥55 ms measured from the nadir of the S-wave until the end of all depolarization deflections in the absence of complete RBBB

5 Arrhythmias

Major

Nonsustained or sustained VT of LBBB morphology with superior axis

Minor

Nonsustained or sustained VT of RVOT configuration, LBBB morphology with inferior axis or with unknown axis

>500 PVCs per 24 h on Holter monitoring

6 Family History

Major

ARVD/C in first-degree relative who meets current TFC

ARVD/C confirmed pathologically at autopsy or surgery in a first-degree relative

Identification of a pathogenic mutation categorized as associated or probably associated with ARVD/C in the patient under evaluation

Minor

History of ARVD/C in first-degree relative in whom it is not possible to determine whether the family member meets current TFC

Premature sudden death (<35 yrs of age) due to suspected ARVD/C in a first-degree relative

ARVD/C confirmed pathologically or by current TFC in second-degree relative

Major criteria count as 2 TFC points, and minor criteria count as 1 TFC point. Definite ARVD/C diagnosis is made with ≥4 TFC points, borderline ARVD/C diagnosis is made with 3 TFC points, and possible ARVD/C diagnosis is made with 2 TFC points.

*Adapted from Marcus et al. (6).

ARVD/C = arrhythmogenic right ventricular dysplasia/cardiomyopathy; BSA = body surface area; CMR = cardiac magnetic resonance; ECG = electrocardiogram; EDV = end-diastolic volume; FAC = fractional area change; LBBB = left bundle branch block; PLAX = parasternal long axis; PSAX = parasternal short axis; PVC = premature ventricular complex; RBBB = right bundle branch block; RV = right ventricular; RVOT = right ventricular outflow tract; SAECG = signal-averaged electrocardiogram; TFC = Task Force Criteria; 2D = 2-dimensional; VT = ventricular tachycardia.

TABLE 2

Clinical Findings of Conditions Considered in the Differential Diagnosis of ARVD/C

Sarcoidosis	Clinical findings: more common in women, African Americans, and Northern European (Scandinavian) whites. Usually nonfamilial disease pattern. May present with extracardiac manifestations (often pulmonary/mediastinal lymphadenopathy, but any organ system may be involved). ECG may show PR-interval prolongation or high-grade atrioventricular block. Useful imaging modalities: x-ray, CT, PET, CMR with LGE Imaging findings: pulmonary granulomas, mediastinal lymphadenopathy, decreased LV function/heart failure, LGE (nonischemic pattern) in the interventricular septum
Myocarditis	Clinical findings: may present with a viral prodrome with fever, myalgia, respiratory and gastrointestinal symptoms, new-onset atrial or ventricular arrhythmias, complete heart block, or acute MI-like syndrome with chest pain, ST-T changes, and elevated cardiac enzymes Useful imaging modalities: echocardiography, CMR with LGE Imaging findings: tissue edema (acute phase), concomitant pericardial involvement, subepicardial patchy myocardial LGE (nonischemic pattern)
DCM	Clinical findings: variable. May be familial. Ventricular arrhythmias usually occur in the context of impaired LV systolic function and morphological abnormalities. Useful imaging modalities: echocardiography, CMR with LGE Imaging findings: dilated LV with reduced function, midwall LGE in the septum
Athlete's Heart	Clinical findings: clinical history is indicative; subjects are typically engaged in intense and repetitive endurance type sports. Physical examination results may show low heart rate, especially in young athletes. Useful imaging modalities: echocardiography with deformation imaging, CMR with LGE Imaging findings: balanced dilation of cardiac chambers, increased ventricular wall thickness (<15 mm), absence of regional ventricular dysfunction or regional wall motion abnormalities, lack of LGE on CMR
Idiopathic RVOT VT	Clinical findings: benign, nonfamilial condition, only 1 VT morphology (LBBB with inferior axis), sinus rhythm ECG normal Useful imaging modalities: echocardiography, CMR with LGE Imaging findings: normal
Brugada Syndrome	Clinical findings: ECG reveals RBBB and persistent ST-segment elevation in the right precordial leads (spontaneous or after provocative drug challenge). Arrhythmias often occur in a sedentary setting (after a meal or at rest because of high vagal tone). Useful imaging modalities: echocardiography, CMR with LGE Imaging findings: normal

CT = computed tomography; DCM = dilated cardiomyopathy; LV = left ventricular; LGE = late gadolinium enhancement; MI = myocardial infarction; PET = positron emission tomography; VT = ventricular tachycardia; other abbreviations as in Table 1.

TABLE 3

Noninvasive Multimodality Imaging in ARVD/C

	TTE	CMR	CT
Spatial resolution	0.5–1 mm*	1–2 mm	0.5 mm
Temporal resolution	15–60 ms	25–50 ms	50–100 ms
Availability	++	−	++
Low cost	++	−	−
Functional analysis	+	++	+
Radiation dose	None	None	Moderate for cine CT (5–10 mSv)
Tissue characterization	N/A	++ (fat/water/fibrosis)	+ (fat)
Remarks	RV imaging requires special emphasis/expertise; cardiac devices are acceptable	Not influenced by habitus; sensitive to arrhythmia; generally not compatible with cardiac devices	Sensitive to arrhythmia; cardiac devices are acceptable

*Axial resolution.

N/A = not available; TTE = transthoracic echocardiography; other abbreviations as in Tables 1 and 2.

TABLE 4

Recommended CMR Protocol for ARVD/C Evaluation*

Sequence	Imaging Plane	Parameters	Comments
Double-inversion recovery TSE/FSE **a.** Axial: with and without fat suppression **b.** Short axis: without fat suppression	**a.** Axial: obtain w6–8 images centered on the LV/RV **b.** Short axis: obtain w6–8 images centered on the LV	TR = 2 R-R intervals, TE = 5 ms (minimum-full) (GE Healthcare, Fairfield, Connecticut), TE 30 ms (Siemens, Munich, Germany), slice thickness = 5 mm, interslice gap = 5 mm, and FOV = 28–34 cm ETL 16–24	This sequence provides optimal tissue characterization of the RV free wall. Prescribe from the pulmonary artery to the diaphragm. Fat suppression improves reader confidence in diagnosis of RV fat infiltration.
SSFP bright blood cine images	Stack of axial images or stack of 4-chamber cine images covering the entire LV and RV. Short axis. RV 3 chamber (optional)	TR/TE minimum, flip angle = 45°–70°, slice thickness = 8 mm, interslice gap = 2 mm FOV = 36–40 cm, 16–20 views per segment. Parallel imaging n = 2 is desirable.	Axial and/or 4-chamber cine images are best to assess RV wall motion. The choice of axial versus 4-chamber view depends on the experience of the observer. RV quantitative analysis is performed on the short-axis cine images.
Gadolinium Is Administered According to Institutional Protocol (Usually 0.15–0.2 mmol/kg)			
TI scout	4 chamber		TI scout sequences or trial TI times to suppress normal myocardium for the right inversion time
Delayed gadolinium imaging (phase-sensitive inversion recovery recommended)	Axial, short axis, 4 chamber, and vertical long axis	TR/TE per manufacturer recommendations flip angle = 20°–25°, slice thickness = 8 mm, interslice gap = 2 mm, FOV = 36–40 cm, no parallel imaging Use phase-sensitive inversion recovery if available	PSIR is more robust and independent of TI time. Optimal for imaging fibrosis. LV epicardial enhancement in the inferolateral wall has been reported in classic ARVD/C and in left dominant forms.

*Reprinted with permission from te Riele et al. (15) (original publisher BioMed Central).

ETL = echo train length; FOV = field of view; FSE = fast spin echo; PSIR = phase-sensitive inversion recovery; SSFP = steady-state free precession; TE = echo time; TI = inversion time; TR = repetition time; TSE = turbo spin echo; other abbreviations as in Tables 1 and 2.